

# Magnetically stabilized exciton-impurity complexes in indium antimonide

I. V. Kavetskaya, N. N. Sibel'din, and V. A. Tsvetkov

*P. N. Lebedev Physics Institute, Russian Academy of Sciences, 117924 Moscow, Russia*

(Submitted 16 February 1994)

Zh. Eksp. Teor. Fiz. **105**, 1714–1732 (June 1994)

The photoluminescence spectra of pure *n*-type indium antimonide crystals ( $N_D - N_A = (0.3-2) \cdot 10^{14} \text{ cm}^{-3}$ ) in a magnetic field of up to 60 kOe were investigated at liquid-helium temperatures and low pumping intensities (less than  $2 \cdot 10^{20} \text{ photons/cm}^2 \cdot \text{sec}$ ). It was found that in a magnetic field, one to three lines of magnetically stabilized exciton-impurity complexes appear, each line corresponding to excitons bound to acceptor atoms of a definite chemical nature. The optical and thermal dissociation energies of exciton-impurity complexes in magnetic fields of different intensities were determined. We show that the principal edge-luminescence line (no magnetic field) is due to transitions of electrons from shallow-donor levels into the valence band.

## 1. INTRODUCTION

It is well known that at low temperatures and moderate excitation levels, the lines of exciton-impurity complexes, as a rule, predominate in the luminescence spectra of even quite pure semiconductors.<sup>1-7</sup> This, however, is not true for indium antimonide. The edge-emission spectrum of this narrow-gap material in the absence of a magnetic field does not contain the luminescence lines of bound excitons (in any case, excitons bound on shallow impurities).<sup>8,9</sup> The point is that the dissociation energy of exciton-impurity complexes in indium antimonide is much too low. In the limit  $m_e/m_h \rightarrow 0$ , the binding energy of an exciton on a neutral donor is  $E_i \approx 0.35E_D$  and the binding energy of an exciton on a neutral acceptor is  $E_i \approx 0.055E_A$  (here  $m_e$  and  $m_h$  are the electron and hole effective masses, respectively, and  $E_D$  and  $E_A$  are the ionization energies of donors and acceptors, respectively).<sup>1</sup> In indium antimonide, the ionization energy of shallow donors is only  $\approx 0.6 \text{ meV}$ , due to the extremely low electron effective mass ( $m_e \approx 0.014m_0$ ). The ionization energy of shallow acceptors is  $E_A \sim 10 \text{ meV}$ . For this reason, for excitons bound to shallow impurities,  $E_i \lesssim 0.5 \text{ meV}$ .

It is well known that a magnetic field stabilizes weakly bound states. Thus the binding energy of an exciton<sup>10-12</sup> and the ionization energy of shallow donors<sup>13-15</sup> are substantially higher in a magnetic field. The fact that with increasing magnetic induction the effective mass of an exciton increases in a direction transverse to the magnetic field<sup>12</sup> makes possible the formation of excitons localized near defects and impurity atoms which could not bind an exciton in the absence of a magnetic field.<sup>16</sup> The influence of a strong magnetic field on the properties of bound excitons was studied theoretically in Refs. 16 and 17. Magnetically stabilized exciton-impurity complexes, just like bound excitons in the absence of a field,<sup>4</sup> have giant oscillator strengths.<sup>16</sup> We experimentally observed magnetically stabilized exciton-impurity complexes in indium antimonide according to the excitation of a characteristic narrow line on the long-wavelength wing of the principal edge-luminescence band in a magnetic field  $H \approx 5-7 \text{ kOe}$ . In a

strong magnetic field, this line dominated the spectrum.<sup>18,19</sup>

In the present paper we present the results of our investigations of the photoluminescence spectra of quite pure *n*-type indium antimonide crystals ( $N_D - N_A = (0.3-2) \cdot 10^{14} \text{ cm}^{-3}$ ) in magnetic fields up to 60 kOe at liquid-helium temperatures and low pumping intensities (less than  $2 \cdot 10^{20} \text{ photons/cm}^2 \cdot \text{sec}$ ). It was found that in a magnetic field, one to three lines of magnetically stabilized exciton-emission complexes appear in the luminescence spectra of the experimental samples, each line corresponding to excitons bound to acceptor atoms of a definite chemical nature. The optical and thermal dissociation energies of exciton-impurity complexes in magnetic fields of different intensities were determined from the experimental data. It was found that in a strong magnetic field, the thermal dissociation energy is lower than the optical dissociation energy, because the electrons liberated by thermal dissociation of complexes occupy shallow-donor levels lying in the tail of the density of states of the conduction band.

No lines of exciton-impurity complexes appeared in the luminescence spectra of the purest experimental samples. Only the principal luminescence line is observed at energies close to the band edge over the entire experimental range of magnetic-field intensities. In a weak magnetic field the diamagnetic shift of the main luminescence line depends nonlinearly on the field intensity. This fact, together with other experimental data, show that the principal edge-luminescence line of sufficiently pure *n*-InSb crystals results from electron transitions from levels of shallow donors into the valence band, and the shape of the line and its spectral position, as established in Ref. 8, are determined by large-scale fluctuations of the impurity potential.

## 2. EXPERIMENTAL PROCEDURE

A  $3.39 \mu\text{m}$  cw He-Ne laser with maximum power of about 15 mW was used in order to investigate luminescence for quasistationary excitation of the samples. The exciting radiation was modulated at a frequency of 1 kHz

TABLE I. The parameters of the experimental samples of  $n$ -InSb and the energies of the maxima of the spectral lines of exciton-impurity complexes at  $H=46$  kOe (dashes indicate that the corresponding lines are not present in the spectrum)

| Sample No. | $n \times 10^{-14}$ , $\text{cm}^{-3}$ | $\mu_e \times 10^{-5}$ , $\text{cm}^2/\text{V} \cdot \text{sec}$ | $\kappa$ | $I_{A_{1,2}}/I_0$ | $I_{A_3}/I_{A_{1,2}}$ | $\hbar\omega_{\text{max}}$ , meV |                   |                    |
|------------|--|--|----------|-------------------|-----------------------|----------------------------------|-------------------|--------------------|
|            |  |  |          |                   |                       | EIC <sub>I</sub>                 | EIC <sub>II</sub> | EIC <sub>III</sub> |
| 1          | 0.3                                    | 7.5  | 0.8      | 0.04              | 0.3                   | 244.9                            | 244.7             | 244.5              |
| 2          | 0.7                                    | 6.0  | 0.7      | 0.03              | 0.8                   | 244.9                            | —                 | 244.5              |
| 3          | 0.96                                   | 6.5  | 0.6      | 0.01              | 5                     | —                                | —                 | 244.5              |
| 4          | 1.0 – 2.0                              | 7.0  | 0.5      | 0.01 – 0.02       | 0.5                   | —                                | 244.7             | —                  |
| 5          | 0.6                                    | 8.0  | 0.6      | —                 | —                     | —                                | —                 | —                  |

Note: N-dash determines the absence of the corresponding lines in the radiation spectrum.

with a mechanical chopper. The laser beam was focused on the wide face of the sample. In most experiments the diameter of the light spot on the surface of the sample was  $\approx 0.3$  mm. The excitation intensity was varied with the help of neutral-density filters.

Recombination radiation was collected either from the laser-illuminated or the opposite face of the sample, analyzed with an MDR-2 monochromator with a 100 lines/mm grating, and recorded either with a Ge:Au photoconductive cell or an InSb photodiode, cooled to  $\sim 100$  K. Since the observation geometry did not appreciably affect the shape of the recorded luminescence spectra, we shall not mention below the face of the sample from which the recombination radiation was collected.

Magnetic fields up to 60 kOe were generated with the help of a superconducting solenoid. Most experiments were performed in the Faraday geometry. Experiments performed in the Voigt geometry did not yield any additional information. For this reason, we present below only the results obtained in the Faraday configuration.

To determine the spectral position of the observed luminescence lines with respect to the energies of the exciton transitions, we measured the magnetoreflexion spectra. In these measurements the radiation from a Globar lamp, modulated with a mechanical chopper, was focused on the sample and the reflected light was analyzed using the same monochromator as in the case of the recombination radiation.

The experimental sample was freely suspended at the center of the working opening of the solenoid, and during the experiment it was immersed in liquid helium. The measurements were performed at  $T=2-4.2$  K. The temperature was regulated by pumping on the helium vapor.

The typical dimensions of the samples were  $5 \times 5 \times (0.1-0.2)$  mm<sup>3</sup>. The wide faces of the samples were perpendicular to the  $\langle 211 \rangle$  axis. After mechanical polishing, the samples were etched in SR-4A polishing etchant. The parameters of the experimental samples are presented in Table I. The electron concentration  $n \approx N_D - N_A$ , where  $N_D$  and  $N_A$  are, respectively, the concentrations of donors and acceptors, and the electron mobility  $\mu_e$ , were measured at  $T=77$  K. The values of  $n$  and  $\mu_e$  presented above and the results of Ref. 20 were used to obtain a rough estimate of the degree of compensation  $\kappa = N_A/N_D$ .

### 3. RESULTS AND DISCUSSION

It has been known since the first investigations of the low-temperature luminescence of  $n$ -InSb that the recombination-radiation spectrum of sufficiently pure crystals of this material in the energy range  $E_g - E_A \lesssim \hbar\omega \lesssim E_g$  (where  $E_g$  is the band gap and  $E_A$  is the ionization energy of shallow acceptors) at low excitation levels contains, besides the principal line (shown in Fig. 1), one or two additional weak lines.<sup>21,22</sup> One of these additional lines, with a maximum near  $\hbar\omega_{\text{max}} \approx 228$  meV, was associated with electron transitions from the conduction band to acceptor levels of zinc, while the other line ( $\hbar\omega_{\text{max}} \approx 224$  meV) was associated with transitions to levels of an unknown impurity.

We observed these lines in our samples also (with the exception of sample N5). Since, however, our  $n$ -InSb samples are extremely pure, the lines under discussion are very weak, so that they were recorded with low spectral resolution. These circumstances, as well as the relatively large

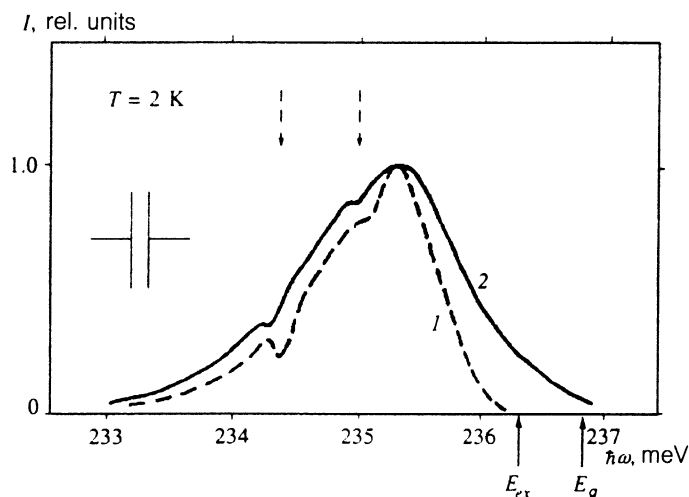


FIG. 1. Principal luminescence lines of samples with  $n \approx 6 \cdot 10^{13} \text{ cm}^{-3}$  (1) and  $n \approx 1.2 \cdot 10^{14} \text{ cm}^{-3}$  (2) at  $H=0$ ,  $T=2$  K, and excitation density  $\approx 10 \text{ W/cm}^2$ . The solid arrows indicate the value of the band gap  $E_g$  and the transition energy  $E_{\text{ex}}$  to the ground state of a free exciton (data of Ref. 23); the dashed lines indicate the position of the absorption lines of atmospheric water vapor.

width of these lines and deformation of the luminescence spectrum due to absorption of the recombination radiation by atmospheric water vapor, make it difficult to determine sufficiently accurately the intensity and spectral position of the maxima of the weak additional lines. In addition, the intensity and position of the maximum of these lines differed somewhat for different samples with essentially identical values of  $n$  and  $\mu_e$  and cut from neighboring parts of the ingot. Summarizing the data obtained on all of the experimental samples, we can conclude that the maximum of the shortest-wavelength line lies in the 226.7–228.0 meV range and the maximum of the longest-wavelength line lies in the 223.5–224.0 range meV. Moreover, the fact that the shape of the short-wavelength line varies from sample to sample suggests that this line is a superposition of at least two lines corresponding to acceptor atoms of different chemical elements, though for the reasons mentioned above, this conclusion requires additional experimental verification on specially doped samples. These acceptors are probably zinc and cadmium, which are usually present in pure indium antimonide and have close ionization energies [ $E_A$  equals, respectively, 9.0 and 10 meV (Refs. 20 and 24)] and whose relative concentrations can be different in samples with a different degree of doping. Germanium and manganese are also shallow acceptors for which  $E_A$  equals 10 and 9.5 meV, respectively.<sup>20,24</sup> With regard to the weak long-wavelength line, it can apparently be inferred from its spectral position that this line is likewise associated with electronic transitions into acceptor levels.

The data on the intensity of the acceptor lines, together with  $n$  and  $\mu_e$ , can be used to characterize the experimental samples. Table I gives the average values of the intensities at the maxima of the short- and long-wavelength acceptor lines. The intensity  $I_{A_{1,2}}$  of the short-wavelength line (the index  $A_{1,2}$  underscores the fact that this line consists of several lines) is given with respect to the intensity of the fundamental line  $I_0$ , and the intensity of the long-wavelength line  $I_{A_3}$  is given with respect to  $I_{A_{1,2}}$ . It should be noted that the intensity of an acceptor line reflects the content of acceptor atoms of definite chemical nature in the sample, while the degree of compensation obtained from the results of electric measurements indicates the total concentration of acceptors (in this case, deep acceptors also) in the crystal. Thus, for example, the concentration of acceptors, estimated using  $n$  and  $\kappa$ , is essentially identical ( $N_A \approx 10^{14} \text{ cm}^{-3}$ ) in samples N4 and N5 (see Table I). At the same time, the acceptor lines are reliably detected in sample N4 and are absent in the case of sample N5.

Additional information about the impurity content in the sample can be obtained by analyzing the shape of the principal emission line, which is determined by the structure of the tails of the density of states.<sup>8,25</sup> Thus, for example, the slope of the long-wavelength wing of the principal line depends on the total concentration of donor and acceptor impurities, and it increases as the total concentration of these impurities decreases.<sup>8</sup> Comparing the shapes of the long-wavelength edge of the principal line of the experimental samples in the absence of a magnetic field showed that samples N1 and N5 have essentially identical

(and the lowest total) impurity concentration among all samples, while sample N2 has the highest total impurity content. These data agree with the values of  $n$  and  $\kappa$  in Table I. At the same time, as one can see from Table I, the luminescence spectrum of sample N5, in contrast to the spectrum of sample N1, does not contain the acceptor emission lines  $A_{1,2}$  and  $A_3$ .

The principal lines of samples N4 and N5 recorded in the absence of a magnetic field and with a low excitation level are displayed in Fig. 1. In contrast to the results of Ref. 26 (where the luminescence of the samples whose impurity composition was close to those of samples N1 and N4 was investigated) the maxima of the principal lines of all of our experimental samples were located near  $\hbar\omega_{\text{max}} \approx 235.3$  meV, while, as one can see from Fig. 1, the lines of different samples had appreciably different shapes and widths. It is entirely natural that the spectra presented in Fig. 1 do not contain the induced emission line<sup>8,9,27</sup> arising in the long-wavelength wing of the principal line (the line B, in the notation adopted in Refs. 26 and 28) at high pumping levels,<sup>28</sup> since the pump levels employed in the experiments described were significantly lower than the level required in order for this line to appear. As for the B line (in the notation of Ref. 26) with a maximum near 231.3 meV, and detected by the authors of Ref. 26, it should be noted that features which could be interpreted as a separate line were observed in the spectra of samples N1, N2, and N4. This line (if it really is one), however, was appreciably weaker than even the acceptor lines, while according to the overall spectrum presented in Ref. 26, the intensity of the B line is comparable to that of the principal band. It should be noted, however, that it is difficult to compare our data directly with the results of Ref. 26, because in Ref. 26 the real spectra of the experimental samples are not presented and the conditions (spectral resolution and range of excitation intensities) under which the B line was observed were not described. Completing our discussion of the luminescence spectra observed in the absence of a magnetic field, we note that here we do not discuss the results of Ref. 29, which are somewhat different from both our data and the results of the works cited above. The point is that the experiments described in Ref. 29 were performed under significantly different excitation conditions and temperatures  $T \gtrsim 5$  K. We shall also not discuss below the results of this work, because when the sample temperature increases from 2 to 4.2 K, the emission lines of the magnetically stabilized exciton-impurity complexes, which were the principal subject of our experiment, vanish.

The spectrum of the sample N5 exhibits the simplest behavior in a magnetic field. This sample has the lowest total concentration of donors and acceptors and the lowest acceptor concentration (according to the values of  $n$  and  $\kappa$  in Table I) of all experimental samples, and most importantly its spectrum has no acceptor lines. A single line (Fig. 2, spectrum 1), whose half-width at first decreases with increasing field intensity and then remains essentially constant for  $H \gtrsim 20$  kOe (Fig. 3), is observed in the spec-

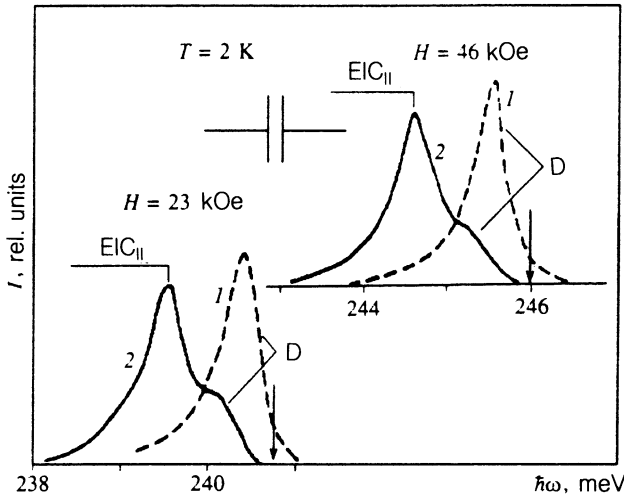


FIG. 2. Luminescence spectra of samples with  $n \approx 6 \cdot 10^{13} \text{ cm}^{-3}$  (1) and  $n \approx 1.5 \cdot 10^{14} \text{ cm}^{-3}$  (2) at  $H=23$  and  $46$  kOe,  $T=2$  K, and excitation density  $\approx 10 \text{ W/cm}^2$ . D—principal luminescence line;  $\text{EIC}_{\text{II}}$ —spectral line of exciton-impurity complexes. The arrows mark the transition energies to the lowest state of diamagnetic excitons, determined according to the position of the “center” (see Fig. 5) of the long-wavelength component of the excitonic magnetoreflexion spectrum.

trum of this sample over the entire experimental range of magnetic field intensities.

As the field intensity increases, the line shifts to higher energies and its intensity decreases somewhat. For low values of  $H$ , the short-wavelength shift of the line maximum is a nonlinear function of the field intensity (Fig. 4a). In a field  $H=20\text{--}30$  kOe, the maximum of the luminescence line lies close to the long-wavelength excitonic magnetoreflexion line. In a stronger field, however, the line is shifted appreciably to the long-wavelength side of the reflection line, the energy splitting between these lines increasing with the field (Figs. 2 and 4a). The values marked with triangles in Fig. 4a correspond to two transitions with the lowest energies in the diamagnetic-exciton (DE) state with identically oriented electron spins. These values were determined from the spectral position of the excitonic magnetoreflexion lines, as shown by the arrow in Fig. 5 for the longest-wavelength reflection line. The two straight lines in Fig. 4a represent the theoretical field-intensity dependences of the energies of these excitonic transitions (Ref. 30).<sup>1)</sup>

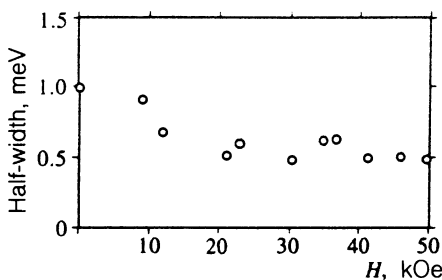


FIG. 3. Half-width of the luminescence line of the sample with  $n \approx 6 \cdot 10^{13} \text{ cm}^{-3}$  as a function of the magnetic-field intensity.

As shown in Ref. 8, the spectral position and shape of the principal edge-emission line of pure  $n$ -InSb samples in the absence of a magnetic field are determined by large-scale fluctuations of the concentration of charged impurities, giving rise to bending of the edges of the allowed bands. The diamagnetic shift (which is a nonlinear function of the field intensity) of the main line for low values of  $H$  (Fig. 4) indicates that this radiation is mainly associated with transitions of electrons occupying shallow donor levels, lying beneath the dips in the conduction band (and not the dips themselves, which are potential wells for itinerant electrons), into spatially separated “hills” of the valence band, which serve as potential wells for holes. The spectral position of this luminescence line in a magnetic field also indicates the donor nature of the line. In both the presence and absence of a magnetic field, the principal line lies at energies less than the energy of an excitonic transition. If, however, in the absence of a magnetic field the binding energies of the donor electron and exciton ( $E_D \approx 0.6 \text{ meV}$  and  $E_{\text{ex}} \approx 0.5 \text{ meV}$ ) are significantly less than the rms electron potential energy  $\gamma$ , which is determined by the fluctuations in the concentration of the charged impurities and which characterizes the average depth of the potential wells<sup>31</sup> that arise (in sample N5,  $\gamma \approx 2 \text{ meV}$ ), then even in a field  $H \sim 10$  kOe  $E_D$ ,  $E_{\text{ex}} \approx \gamma$  [ $E_D \approx 2 \text{ meV}$  for  $H \sim 10$  kOe (Refs. 15 and 20)], while in stronger fields the ionization energies of the donors and excitons are much greater than  $\gamma$ . Moreover, as the ionization energy of the donors increases, the rms potential can decrease as a result of recharging of impurities accompanying excitation of the sample. In the absence of a field the energy of the principal line measured from the band edge is therefore determined mainly by the depth and spatial extent of the fluctuation potential wells, while in a sufficiently strong field it is determined by the ionization energy of the donors. Thanks to this circumstance, the observed spectral position of the principal line in a magnetic field also points to the fact that it is of a donor nature.

It is possible, however, that in the absence of a field, the radiation resulting from the recombination of itinerant electrons occupying the dips of the conduction band makes a definite contribution to the short-wavelength wing of the principal line. This is indicated by the decrease in the width of the line with increasing magnetic field intensity (Fig. 3). This decrease in the linewidth can be explained by electron localization on donor centers as a result of magnetic-field-induced freezing out<sup>32</sup> associated with the increase in the ionization energy of the donors. On the other hand, in a magnetic field the transition probabilities of electrons from donor centers into neighboring centers decrease due to the decrease in the overlap of the “tails” of the donor wave functions,<sup>31</sup> and since there is an energy spread from the donor levels, an increase in the field intensity should likewise result in narrowing of the luminescence line as a result of the recombination of donor electrons.

The principal luminescence lines of the other experimental samples also behave similarly with increasing magnetic field intensity.<sup>2)</sup> They shift to the short-wavelength side and become narrower and weaker. For sample N4, the

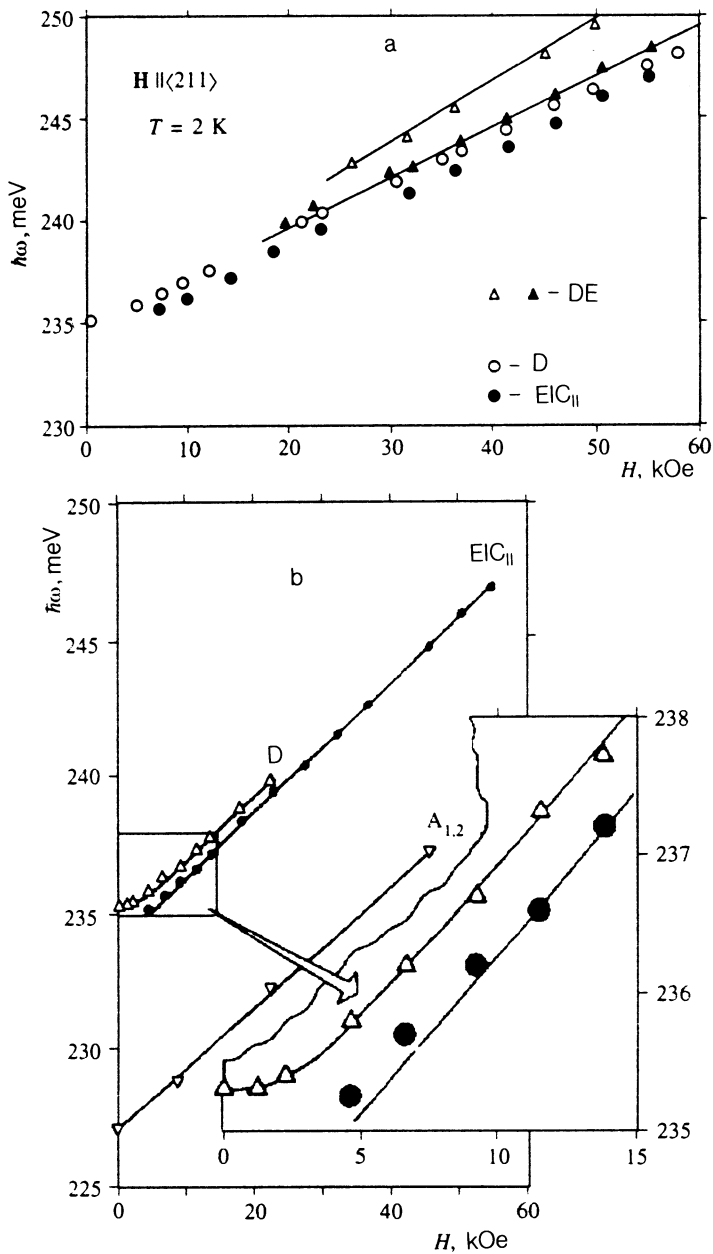


FIG. 4. Spectral position of the two longest-wavelength excitonic magnetoreflexion lines and the maxima of the luminescence lines as a function of the magnetic field intensity: DE—magnetoreflexion, D—principal luminescence line, EIC<sub>II</sub>—spectral line of exciton-impurity complexes of a sample with  $n \approx 1.2 \cdot 10^{14} \text{ cm}^{-3}$ ,  $A_{1,2}$ —acceptor line. (a) the line D of a sample with  $n \approx 6 \cdot 10^{13} \text{ cm}^{-3}$ ; straight lines—transition energies into the two lowest states of diamagnetic excitons (theory); (b) sample with  $n \approx 1.2 \cdot 10^{14} \text{ cm}^{-3}$ .

dependence of the spectral position of the maximum of the donor line on the field intensity is displayed in Fig. 4b (curve D). As one can see from this figure, in a weak field the diamagnetic shift of the maximum of this line is a nonlinear function of the field, while thanks to the more than two orders of magnitude lower diamagnetic susceptibility, the maximum of the acceptor line ( $A_{1,2}$  curve) observed in this sample shifts with a constant rate over the entire range of magnetic field intensity. The donor line basically decreased in intensity in a magnetic field all the more strongly with increasing field intensity, the stronger the emission lines of the exciton-impurity complexes. Even for samples with similar parameters, for example, the samples N4 cut from neighboring parts of the same ingot and having essentially identical  $n$  and  $\mu_e$ , the intensities of the donor lines in a strong magnetic field could differ appreciably, as can be seen by comparing the spectra represented by the solid lines in Figs. 2 and 5.

The lines of exciton-impurity complexes are excited in

the luminescence spectra of samples N1–N4 in a magnetic field. Thus, a line of exciton-impurity complexes appears in the long-wavelength wing of the principal band in the spectrum of sample N4 in fields  $H = 5\text{--}7 \text{ kOe}$ .<sup>18,19</sup> The intensity of this line increases with the field intensity, and in strong fields it dominates the spectrum (Figs. 2 and 5, the line EIC<sub>II</sub>). In a strong magnetic field, the half-width of this line is 0.2–0.4 meV. In a weak field, the short-wavelength shift of the maximum of the line of the exciton-impurity complexes is a nonlinear function of the field intensity (inset in Fig. 4b), while in a sufficiently strong field a linear dependence is observed (Figs. 4a and b). The energy interval between the spectral position of the line maximum for exciton-impurity complexes and the position of the long-wavelength component of the excitonic magnetoreflexion spectrum (the optical dissociation energy of exciton-impurity complexes) in strong magnetic fields increases slightly as the intensity of the field increases (Fig.

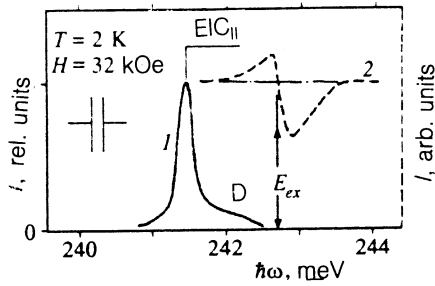


FIG. 5. Luminescence spectrum (1) and long-wavelength component of the excitonic magnetoreflexion spectrum (2) of a sample with  $n \approx 1.2 \cdot 10^{14} \text{ cm}^{-3}$  in a magnetic field  $H = 32 \text{ kOe}$  ( $T = 2 \text{ K}$ ). The arrow marks the transition energy to the lowest state of the diamagnetic exciton.

4a):  $E_i^{op} \approx 1.2 \text{ meV}$  for  $H = 23 \text{ kOe}$  and  $E_i^{op} \approx 1.4 \text{ meV}$  for  $H = 46 \text{ kOe}$ .

In the other samples, one to three lines of exciton-impurity complexes stabilized by a magnetic field are observed. These lines behave as a function of the field intensity qualitatively identically to the line of exciton-impurity complexes of sample N4, but they are excited in a field of different intensity. One line of exciton-impurity complexes, the line with the longest wavelength (the line  $\text{EIC}_{\text{III}}$ ), which is excited in fields  $H \sim 14 \text{ kOe}$ , is observed in sample N3. Two lines of exciton-impurity complexes—the longest-wavelength line ( $\text{EIC}_{\text{III}}$ ) at  $H \sim 9 \text{ kOe}$  and the shortest-wavelength line ( $\text{EIC}_I$ ) at  $H \sim 18 \text{ kOe}$ —appear successively in the spectrum of sample N2 with increasing magnetic field intensity. The luminescence spectrum of sample N1 is distinguished by an especially rich collection of spectral lines. All three observed lines of exciton-impurity complexes are observed for this sample:  $\text{EIC}_{\text{III}}$ ,  $\text{EIC}_{\text{II}}$ , and  $\text{EIC}_I$ . These lines appeared successively in the luminescence spectrum starting with  $H = 7\text{--}9 \text{ kOe}$ . However, it is difficult to say which of the two long-wavelength lines  $\text{EIC}_{\text{III}}$  or  $\text{EIC}_{\text{II}}$  appears at the lower field intensity. However, these lines were reliably resolved in the field  $H = 14 \text{ kOe}$ : The splitting between their peaks was  $\approx 0.2 \text{ meV}$  and remained constant when the magnetic field intensity was increased further. The  $\text{EIC}_I$  line first appeared at  $H \sim 37 \text{ kOe}$ . All three lines can be seen clearly at  $H = 46 \text{ kOe}$ ; the splitting between the peaks of the neighboring lines was  $\approx 0.2 \text{ meV}$  and was independent of the field intensity for  $H > 46 \text{ kOe}$ . The luminescence spectra of samples N1–N4 in the field  $H = 46 \text{ kOe}$  are displayed in Fig. 6, and the spectral position of the line maxima of exciton-impurity complexes is given in Table I.

As we have noted previously (for the  $\text{EIC}_{\text{II}}$  line), the

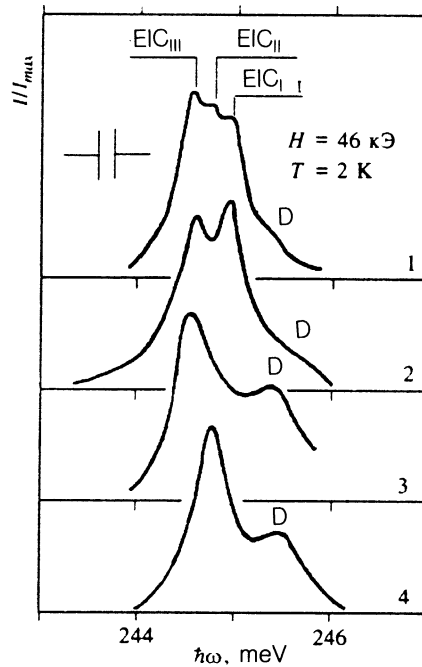


FIG. 6. Luminescence spectra of samples with  $n \approx 3 \cdot 10^{13} \text{ cm}^{-3}$  (1),  $\approx 7 \cdot 10^{13} \text{ cm}^{-3}$  (2),  $\approx 9.6 \cdot 10^{13} \text{ cm}^{-3}$  (3), and  $1.5 \cdot 10^{14} \text{ cm}^{-3}$  (4) in a magnetic field  $H = 46 \text{ kOe}$ . The excitation intensity is  $\approx 10 \text{ W/cm}^2$  and  $T = 2 \text{ K}$ . For each spectrum the intensity at the maximum  $I_{\text{max}} = 1$ . D—principal luminescence line;  $\text{EIC}_I$ ,  $\text{EIC}_{\text{II}}$ , and  $\text{EIC}_{\text{III}}$  are lines of exciton-impurity complexes.

observed emission is due to recombination of electrons and holes in exciton-impurity complexes, consisting of a diamagnetic exciton bound to a neutral shallow acceptor.<sup>19</sup> Correlation of the intensities of the acceptor lines to the presence of lines of exciton-impurity complexes in the spectra of different samples (see Table I) and analysis of the experimental data described above confirm and make it possible to elaborate this hypothesis. Thus, neither acceptor lines nor the lines of exciton-impurity complexes are observed in sample N5. Sample N3 is characterized by relatively weak acceptor emission  $A_{1,2}$  and the strongest emission  $A_3$ , owing to recombination of electrons with holes located on acceptors with deep energy levels. For this reason, the isolated  $\text{EIC}_{\text{III}}$  line observed in this sample can be attributed to excitons bound to acceptors responsible for the  $A_3$  emission. Continuing the discussion in the same vein, we can conclude that the  $\text{EIC}_I$  and  $\text{EIC}_{\text{II}}$  lines belong to excitons localized on acceptor atoms of different chemical elements, to which the compound line  $A_{1,2}$  corresponds (see the discussion at the beginning of this section). Such referencing of the  $\text{EIC}_I$ ,  $\text{EIC}_{\text{II}}$ , and  $\text{EIC}_{\text{III}}$  lines of exciton-impurity complexes to the acceptor lines  $A_{1,2}$  and  $A_3$ , respectively, is in general agreement with all data presented in Table I.

The foregoing picture is also supported by the fact that the dissociation energy of exciton-impurity complexes increases (from  $\text{EIC}_I$  to  $\text{EIC}_{\text{III}}$ , Fig. 6) when excitons are bound to deeper acceptors, and that the intensity of the magnetic field stabilizing the corresponding exciton-impurity complex increases as the dissociation energy de-

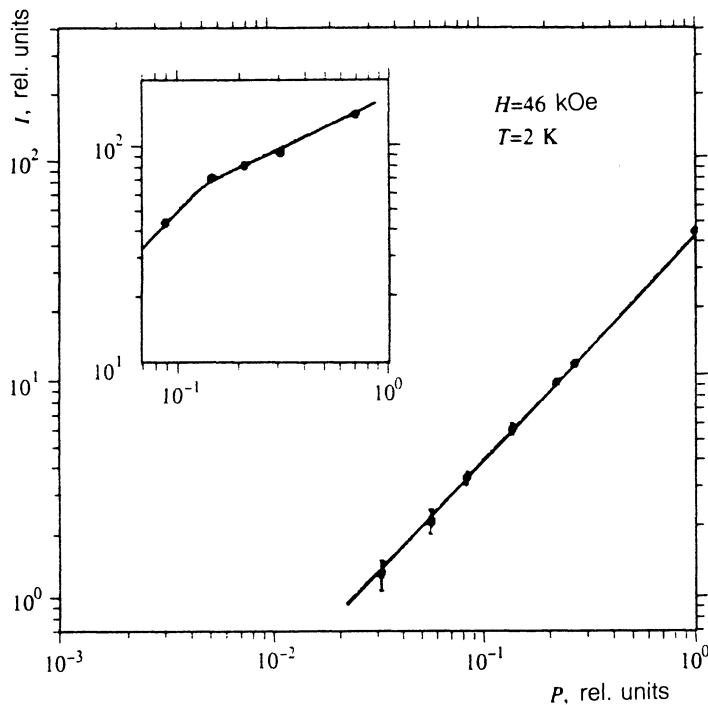


FIG. 7. Intensity of spectral line of exciton-impurity complexes as a function of laser pumping intensity with  $\lambda = 3.39 \mu\text{m}$  with low levels of excitation (maximum excitation density  $\approx 10 \text{ W/cm}^2$ ).  $H = 46 \text{ kOe}$ ,  $T = 2 \text{ K}$ . Inset: Same curve at high levels of pumping with a  $1.06 \mu\text{m}$  laser (maximum excitation intensity  $\approx 480 \text{ W/cm}^2$ ).

creases. As is evident from what we have said above, the latter feature is clearly seen for samples N1 and N2. It would be surprising, however, if a line due to excitons bound to acceptor atoms of a definite chemical nature appeared in the luminescence spectra of different samples at exactly the same magnetic-field intensities. The point is that the lines of the complexes appear against the background of the principal luminescence band, whose intensity is significant and varies from sample to sample, while the intensity of a particular line of bound excitons depends on the concentration of the corresponding acceptors, which is different in different samples. The fact that neighboring lines of exciton-impurity complexes are superimposed also makes it difficult to determine when a new line appears in the spectrum.

To summarize, we can conclude that magnetic-field-stabilized exciton-impurity complexes formed by excitons bound to chemically different shallow acceptors can form in indium antimonide. These complexes give in the luminescence spectra characteristic narrow lines which are significantly stronger (tens of times stronger in our experimental samples) than the corresponding acceptor lines. We emphasize the fact that in our experiments, the exciton-impurity complexes were observed in samples of extremely pure  $n\text{-InSb}$ , and in spite of the fact that these samples had essentially identical concentrations of the principal and compensating impurities, as determined from electric measurements ( $n$  and  $\mu_e$ , presented in Table I), the number and intensity of lines of exciton-impurity complexes in their luminescence spectra in a magnetic field were significantly different. Thus, the lines of magnetically stabilized exciton-impurity complexes can serve as a very sensitive indicator for determining the abundance and chemical nature of shallow acceptors in indium antimonide.

We now discuss the influence of the excitation intensity and temperature on the intensity of the radiation emitted by exciton-impurity complexes. The dependence of the luminescence intensity of the complexes on the level of excitation was investigated in detail for samples N4 at  $T = 2 \text{ K}$ . This dependence, obtained in the field  $H = 46 \text{ kOe}$ , for one sample whose donor line in a strong magnetic field was weak (the ratio of the intensities of the donor line and the line of the complexes is approximately the same as in the spectrum shown in Fig. 5) is shown in Fig. 7. For relatively low pumping levels, the luminescence intensity of exciton-impurity complexes increases linearly with the excitation intensity. For high excitation levels this dependence is significantly weaker (inset in Fig. 7).<sup>3)</sup> The intensity of complexes with intense pumping actually increases even more slowly than shown in the inset in Fig. 7. Experiments performed with an additional slit positioned horizontally in front of the entrance (vertical) slit of the monochromator showed that the intensity of the luminescence line of the complexes increases under strong excitation mainly due to emission from regions of the crystal far from the laser focus. Moreover, under intense pumping the luminescence spectrum acquires a line of a magnetically stabilized electron-hole liquid. This line is superimposed on the emission line of the exciton-impurity complexes.<sup>18)</sup> Similar behavior of the radiative intensity from complexes as a function of the pumping level was also observed for other values of the magnetic field intensity.

To study the effect of the excitation level on the luminescence intensity of sample N1, in whose emission spectrum three lines of exciton-impurity complexes are clearly resolved in a field  $H \approx 42 \text{ kOe}$ , the pumping intensity was varied both by defocusing the laser beam on the surface of the sample and with the help of neutral-density filters. The experiments showed that the ratio of the line intensities of

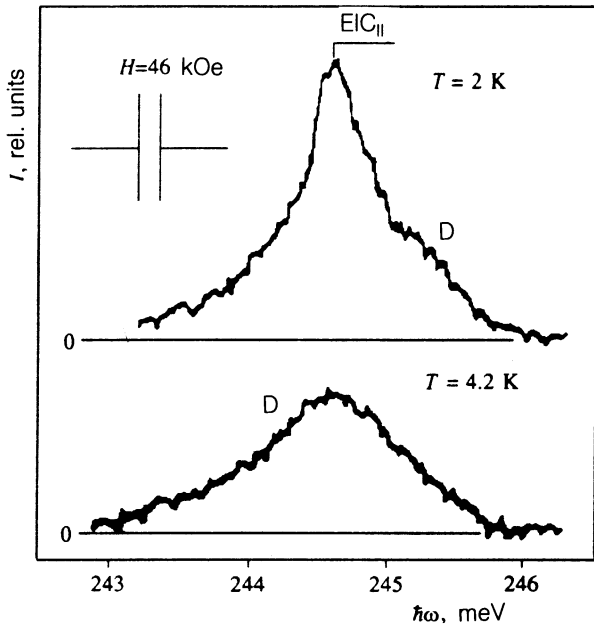


FIG. 8. Spectra of a sample with  $n \approx 1.5 \cdot 10^{14} \text{ cm}^{-3}$  in a field  $H = 46 \text{ kOe}$  at temperatures  $T = 2 \text{ K}$  and  $4.2 \text{ K}$ . The excitation intensity  $\approx 10 \text{ W/cm}^2$ .

the complexes remains constant as a function of the excitation density.

It should be noted that the character of the dependence of the intensity of the lines of magnetically stabilized exciton-impurity complexes on the pumping level completely eliminates amplification as a possible factor in the appearance of these lines in the emission spectrum, especially since the lines of the complexes are observed with pumping intensities almost three orders of magnitude lower than the induced emission line in the absence of a magnetic field.<sup>9</sup> At the same time, the lasing threshold of an InSb laser is not more than an order of magnitude lower in a magnetic field.<sup>33-35</sup> It is thus obvious that the bound-exciton lines that we observed are completely unrelated to the B line studied in Refs. 26 and 28.

The temperature dependences of the spectral composition of recombination radiation were investigated at low excitation intensity ( $\approx 10 \text{ W/cm}^2$ ) for samples No. 4, whose principal line had an appreciable intensity at  $T = 2 \text{ K}$  in a strong magnetic field. As the temperature increased from  $T = 2 \text{ K}$ , the intensity of the line of exciton-impurity complexes decreased gradually, while the intensity of the donor line increased somewhat and its maximum shifted to longer wavelengths. Close to  $T \approx 4.2 \text{ K}$ , the donor line dominated the luminescence spectrum. The spectra of the sample N4 in a magnetic field  $H = 46 \text{ kOe}$  at  $T = 2 \text{ K}$  and  $4.2 \text{ K}$  are shown in Fig. 8. The intensities of the lines of exciton-impurity complexes are shown in Fig. 9 as a function of the inverse temperature for three values of the magnetic field intensity. The luminescence spectrum of sample N1 exhibited similar behavior as a function the temperature. As the temperature increases, the intensities of all three lines of exciton-impurity complexes observed in this sample decreased, and the lines ultimately vanished near

$T \approx 4 \text{ K}$ . Unfortunately, we were unable to measure the temperature dependence of the intensity of each of these lines.

To analyze these results, we employ the stationary solution of the well-known equations describing the kinetics of a nonequilibrium two-component system consisting of free and bound excitons.<sup>36</sup> We shall not write out the general expression describing the dependence of the concentration of exciton-impurity complexes on the excitation level and temperature, but rather we present the formulas for the cases of weak and strong pumping of interest to us. At low pumping levels ( $g\tau_i \ll N_A + n^*$ ), the concentration of exciton-impurity complexes varies according to

$$N_i = \frac{N_A}{N_A + n^*} g\tau_i, \quad (1)$$

and at high excitation intensities ( $g\tau_i \gg N_A + n^*$ ) it is described by

$$N_i = N_A \left( 1 - \frac{N_A + n^*}{g\tau_i} \right). \quad (2)$$

Here we have introduced the notation

$$n^* = \frac{\tau_i}{\tau_{ex}} \left[ \frac{1}{\sigma v_T \tau_i} + \frac{g_A g_{ex}}{g_i} \left( \frac{M_d k T}{2\pi \hbar^2} \right)^{3/2} \exp\left(-\frac{E_i}{kT}\right) \right]. \quad (3)$$

In (1)–(3),  $g$  is the rate of volume generation of excitons;  $N_A$  is the concentration of impurity centers on which complexes form;  $g_A$ ,  $g_{ex}$ , and  $g_i$  are the corresponding degeneracy factors;  $M_d$  is the effective mass of the excitonic density of states, which in a magnetic field is a combination of longitudinal and transverse masses;  $\tau_i$  and  $\tau_{ex}$  are the lifetimes of bound and free excitons, respectively;  $\sigma$  is the cross section for binding of excitons to centers;  $v_T$  is the thermal velocity of the exciton; and  $E_i$  is the dissociation energy of exciton-impurity complexes. From Eq. (1),<sup>36-38</sup>

$$I_i = \frac{J_0}{1 + C T^{3/2} \exp(-E_i/kT)}, \quad (4)$$

which describes the temperature dependence of the radiative intensity of exciton-impurity complexes at low excitation levels. In this expression,  $J_0$  is the luminescence intensity of complexes at  $T = 0 \text{ K}$  and

$$C = \frac{g_A g_{ex}}{g_i} \left( \frac{M_d k}{2\pi \hbar^2} \right)^{3/2} \frac{\sigma v_T \tau_i}{1 + \sigma v_T \tau_{ex} N_A}. \quad (5)$$

As one can see from Eqs. (1) and (2), in accordance with the results presented in Fig. 7, at low pumping levels the concentration of exciton-impurity complexes (and hence the line intensity of the complexes) is proportional to the generation rate  $g$  (excitation intensity), while at high pumping levels the concentration saturates, approaching that of the impurity centers  $N_A$  for large  $g$ . An analysis of the temperature dependence of the line intensity of complexes with the help of (4) is presented in Fig. 9. The values of the adjustable parameters  $E_i$  and  $C$  obtained from this analysis are presented in the caption to this figure. Because the spectral line due to the complexes is superimposed on the principal line, there is a certain arbitrariness



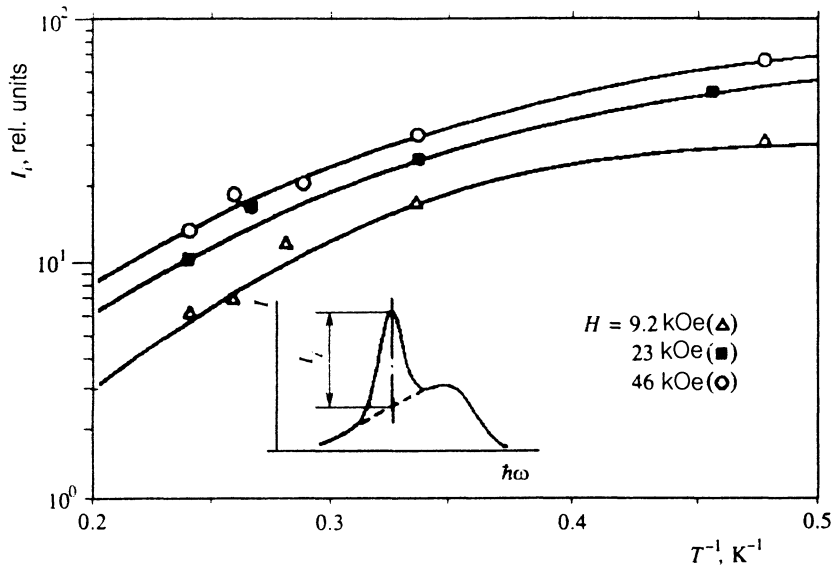


FIG. 9. Intensity of the luminescence line of exciton-impurity complexes versus the inverse temperature (the ratio of  $J_i$  is not constant for different  $H$ ). The solid curves were calculated according to (4) with the following values of the fitting parameters: for  $H=9.2$  kOe:  $E_i=1.1$  meV,  $C=12$  K $^{-3/2}$ ;  $H=23$  kOe:  $E_i=0.6$  meV,  $C=4.0$  K $^{-3/2}$ ;  $H=46$  kOe:  $E_i=0.6$  meV,  $C=3.6$  K $^{-3/2}$ . Inset: Method for determining  $J_i$ .

in choosing the intensity with respect to which the line intensity of the complexes should be measured (see inset in Fig. 9). Both  $I_i$  and the adjustable parameters are therefore not measured very accurately (especially at temperatures close to  $T \approx 4$  K). The adjustable parameters are determined to within about 40%. It can nonetheless be concluded that Eq. (4) describes satisfactorily the observed temperature dependence of  $I_i$ .

The fitting parameter  $E_i$ , which is the thermal dissociation energy  $E_i^T$  of the complexes ( $E_i^T \approx 1.1$  meV in the field  $H=9.2$  kOe), is probably close to the optical dissociation energy. When the field intensity increases to  $H=23$  kOe, this parameter decreases to  $E_i^T \approx 0.6$  meV, after which it remains constant as the field intensity increases further ( $E_i^T \approx 0.6$  meV at  $H=46$  kOe; see caption to Fig. 9), while the optical dissociation energy of the complexes increases from  $E_i^{op} \approx 1.2$  meV at  $H=23$  kOe to  $E_i^{op} \approx 1.4$  meV at  $H=46$  kOe. Thus, in a sufficiently strong field the thermal dissociation energy of the complexes is significantly lower than the optical dissociation energy. However, the values obtained for  $E_i^T$  approximately correspond to the energy splitting between the line maxima of the complexes and the donor line (see Figs. 2, 4b, and 8). It can therefore be conjectured that electrons liberated by thermal dissociation of exciton-impurity complexes are transferred to shallow donor levels in the tail of the density of states of the conduction band. This is also suggested by the increase in the intensity of the donor emission with increasing temperature. For this dissociation mechanism for the complexes,  $E_i^T$  is determined by the position of the electron quasi-Fermi level, which in a relatively weak field decreases with increasing field intensity, as indicated directly by the narrowing of the donor luminescence line (Fig. 3).

Even in this case, the expression (4) with a different factor  $C$  multiplying the exponential, can describe, under certain conditions, the temperature dependence of the emission intensity of exciton-impurity complexes. This factor, however, just like the factor  $C$  determined by Eq. (5), must contain a set of parameters that describe the kinetics

of formation and dissociation of complexes, as well as the recombination kinetics of electron and holes in the non-equilibrium system under consideration. Since with increasing field intensity, the factor  $C$  behaves like  $E_i^T$ , i.e., it first decreases rapidly (from  $C=12$  K $^{-3/2}$  at  $H=9.2$  kOe to  $C=4.0$  K $^{-3/2}$  at  $H=23$  kOe), after which it remains essentially constant ( $C=3.6$  K $^{-3/2}$  at  $H=46$  kOe), it can be conjectured that its value is also determined by the position of the electron quasi-Fermi level. This probably means that the coefficient  $C$  is determined by the behavior of electrons occupying the levels of shallow donors. The foregoing dissociation process in complexes corresponds to the inverse process of capture of donor electrons by acceptor ions  $A^+$ . The rate of this process must be determined by the capture cross section of electrons by  $A^+$  centers and by the average thermal velocity of the donor electrons, similar to the manner in which the rate of binding of excitons to impurity centers is determined by the capture coefficient  $\beta = \sigma v_T$ . It is evident from Eq. (5), obtained by analyzing the kinetics of a system consisting of free and bound excitons, that the coefficient  $C$  is a monotonic function of  $\beta$ . On the basis of the physical meaning of this coefficient, it can be expected that even in our case there should be analogous dependence of  $C$  on the capture coefficient. The average thermal velocity of donor electrons is determined by the transition probabilities of electrons from neutral donors to neighboring ionized donor centers, and the transition probabilities are proportional to the corresponding squared overlap integrals. The compression of the wave functions of donor electrons in a magnetic field<sup>31,32</sup> should therefore cause the constant  $C$  to decrease with increasing field intensity.

Our results thus show that the magnetically stabilized exciton-impurity complexes observed in indium antimonide are excitons bound to neutral acceptors. In addition, these complexes are formed in two steps: first, a neutral acceptor  $A^0$  binds a hole and is converted to an  $A^+$  center. An electron located on a neighboring donor is then trapped by this center.

## CONCLUSIONS

Our investigations of the photoluminescence spectra of pure samples of *n*-type indium antimonide have yielded additional proof of the formation of magnetically stabilized exciton-impurity complexes, which we observed previously,<sup>18,19</sup> in an excited crystal. These complexes consist of an exciton bound to a neutral shallow acceptor. The optical and thermal dissociation energies of the complexes were measured. The difference between the thermal and optical dissociation energies (in a strong magnetic field, the thermal dissociation energy is approximately half the optical dissociation energy) is explained by the participation of donor states in the formation and dissociation of exciton-impurity complexes. It was observed that one to three lines of exciton-impurity complexes appear in the luminescence spectra of the experimental samples in a magnetic field. Each line corresponds to excitons bound to shallow acceptors of a definite chemical nature. Thanks to the narrowness, high intensity, and well-defined position in the spectrum, the lines of magnetically stabilized complexes are a sensitive indicator of acceptor impurities with shallow levels in indium antimonide and can be used to identify such impurities. However, in order to realize this possibility in practice, further investigations must be carried out on samples whose impurity composition is known beforehand.

We are deeply grateful to L. V. Keldysh and A. L. Efros for their interest in this work and for discussion of the results, N. V. Zamkovets for assistance in performing the experiments, and V. S. Ivleva, M. N. Kevorkov, and A. N. Popkov for providing the samples.

Financial support of this work was provided by the Russian Fund for Fundamental Research (Grant No. 93-02-2356).

<sup>1</sup>We thank A. L. Efros for providing us with the numerical results employed in constructing these curves.

<sup>2</sup>Further, in order to underscore the fact that the donor line is the principal line in the luminescence spectrum in the absence of a magnetic field, we shall sometimes also call the principal line a donor line in a magnetic field, although in a magnetic field it can be much weaker than the lines of exciton-impurity complexes.

<sup>3</sup>The results presented in the inset in Fig. 7 were obtained by exciting the sample with Nd<sup>3+</sup> YAG laser radiation at  $\lambda = 1.06 \mu\text{m}$ . In this experiment the excitation was modulated with a 10% duty cycle in order to prevent overheating of the sample. In all other experiments the duty cycle was 50%.

<sup>1</sup>M. A. Lampert, Phys. Rev. Lett. **1**, 450 (1958).

<sup>2</sup>J. R. Haynes, Phys. Rev. Lett. **4**, 361 (1960).

<sup>3</sup>D. G. Thomas and J. J. Hopfield, Phys. Rev. **128**, 2135 (1962).

<sup>4</sup>E. I. Rashba and G. E. Gurgenshivili, Fiz. Tverd. Tela **4**, 1029 (1962) [Sov. Phys. Solid State **4**, 759 (1962)].

<sup>5</sup>E. I. Rashba, Fiz. Tekh. Poluprovodn. **8**, 1241 (1974) [Sov. Phys. Semicond. **8**, 807 (1974)].

<sup>6</sup>P. J. Dean and D. C. Herbert, Top. Curr. Phys. **14**, 55 (1979).

- <sup>7</sup>E. I. Rashba and M. D. Sturge (eds.), *Excitons, Modern Problems in Condensed Matter Sciences*, North-Holland, Amsterdam, 1982, Vol. 2.
- <sup>8</sup>I. V. Kavetskaya, N. B. Kakhramanov, N. N. Sibel'din, and V. A. Tsvetkov, Zh. Eksp. Teor. Fiz. **100**, 2053 (1991) [Sov. Phys. JETP **73**, 1139 (1991)].
- <sup>9</sup>I. V. Kavetskaya, N. N. Sibel'din, and V. A. Tsvetkov, Fiz. Tverd. Tela **34**, 857 (1992) [Sov. Phys. Solid State **34**, 458 (1992)].
- <sup>10</sup>R. J. Elliott and R. Loudon, J. Phys. Chem. Solids **8**, 382 (1959).
- <sup>11</sup>R. J. Elliott and R. Loudon, J. Phys. Chem. Solids **15**, 196 (1960).
- <sup>12</sup>L. P. Gor'kov and I. E. Dzyaloshinskii, Zh. Eksp. Teor. Fiz. **53**, 717 (1967) [Sov. Phys. JETP **26**, 449 (1968)].
- <sup>13</sup>Y. Yafet, R. W. Keyes, and E. N. Adams, J. Phys. Chem. Solids **1**, 137 (1956).
- <sup>14</sup>D. M. Larsen, J. Phys. Chem. Solids **29**, 271 (1968).
- <sup>15</sup>A. Raymond, T. L. Robert, W. Zawadzki *et al.*, J. Phys. C **17**, 2381 (1984).
- <sup>16</sup>V. A. Kharchenko, Zh. Eksp. Teor. Fiz. **83**, 1971 (1982) [Sov. Phys. JETP **56**, 1140 (1982)].
- <sup>17</sup>F. Dujardin, B. Stebe, and G. Munschy, Phys. Status Solidi B **141**, 559 (1987).
- <sup>18</sup>I. V. Kavetskaya, Ya. Ya. Kost', N. N. Sibel'din, and V. A. Tsvetkov, Pis'ma Zh. Eksp. Teor. Fiz. **36**, 254 (1982) [JETP Lett. **36**, 311 (1982)].
- <sup>19</sup>I. V. Kavetskaya and N. N. Sibel'din, Pis'ma Zh. Eksp. Teor. Fiz. **38**, 67 (1983) [JETP Lett. **38**, 76 (1983)].
- <sup>20</sup>L. B. Litvak-Gorskaya, Doctoral Dissertation, Leningrad Polytechnical Institute, Leningrad, 1983.
- <sup>21</sup>C. Benoit à la Guillaume and P. Lavallard, in *Proceedings of the 6th International Conference on Phys. Semicond., Exeter, 1962, Inst. Phys. and Phys. Soc., London (1962)*, p. 875.
- <sup>22</sup>A. Mooradian and H. Y. Fan, Phys. Rev. **148**, 873 (1966).
- <sup>23</sup>L. M. Kanskaya, S. I. Kokhanovskii, and R. P. Seisyan, Fiz. Tekh. Poluprovodn. **13**, 2424 (1979) [Sov. Phys. Semicond. **13**, 1420 (1979)].
- <sup>24</sup>V. S. Ivleva, I. N. Kurilenko, L. B. Litvak-Gorskaya, A. N. Popkov, and V. I. Selyanina, in *Abstracts of the 3rd All-Union Conference on Physical and Chemical Foundations of Doping of Semiconductor Materials*, Moscow (1975), p. 11.
- <sup>25</sup>M. S. Bresler, O. B. Gusev, and A. O. Stepanov, Fiz. Tekh. Poluprovodn. **17**, 1195 (1983) [Sov. Phys. Semicond. **17**, 755 (1983)].
- <sup>26</sup>R. P. Seisyan and Sh. U. Yuldashev, Fiz. Tverd. Tela **30**, 12 (1988) [Sov. Phys. Solid State **30**, 6 (1988)].
- <sup>27</sup>M. S. Bresler, O. B. Gusev, and A. O. Stepanov, Fiz. Tverd. Tela **28**, 1387 (1986) [Sov. Phys. Solid State **28**, 781 (1986)].
- <sup>28</sup>V. I. Ivanov-Omskii, S. I. Kokhanovskii, R. P. Seisyan *et al.*, Fiz. Tekh. Poluprovodn. **17**, 532 (1983) [Sov. Phys. Semicond. **17**, 334 (1983)].
- <sup>29</sup>N. A. Kalugina, Author's Abstract, Candidate's Dissertation, Institute of the Physics of Semiconductors, Siberian Branch of the USSR Academy of Sciences, Novosibirsk (1986).
- <sup>30</sup>B. L. Gel'mont, R. P. Seisyan, A. L. Efros, and A. V. Varfolomeev, Fiz. Tekh. Poluprovodn. **11**, 238 (1977) [Sov. Phys. Semicond. **11**, 139 (1977)].
- <sup>31</sup>B. I. Shklovskii and A. L. Efros, *Electronic Properties of Doped Semiconductors*, Springer-Verlag [English translation] N.Y. (1984).
- <sup>32</sup>R. J. Sladek, J. Phys. Chem. Solids **5**, 157 (1958).
- <sup>33</sup>J. I. Pankove, *Optical Processes in Semiconductors*, Prentice-Hall, Englewood Cliffs (1971).
- <sup>34</sup>S. P. Grishchikina, Trudy FIAN **89**, 59 (1976).
- <sup>35</sup>N. A. Kalugina and E. M. Skok, Fiz. Tverd. Tela **27**, 528 (1985) [Sov. Phys. Solid State **27**, 324 (1985)].
- <sup>36</sup>B. M. Ashkinadze, S. M. Ryvkin, and I. D. Yaroshetskii, Fiz. Tekh. Poluprovodn. **3**, 535 (1969) [Sov. Phys. Semicond. **3**, 455 (1969)].
- <sup>37</sup>P. J. Dean, Phys. Rev. **157**, 655 (1967).
- <sup>38</sup>D. Bimbarly, M. Sondergeld, and E. Grobe, Phys. Rev. B **4**, 3451 (1971).

Translated by M. E. Alferieff